JOURNAL OF AIRCRAFT
Vol. 40, No. 3, May–June 2003

Dynamic Aeroelastic Response of Aircraft Wings Modeled as Anisotropic Thin-Walled Beams

Zhanming Qin* and Liviu Librescu†
Virginia Polytechnic Institute and State University, Blacksburg, Virginia 24061-0219

The dynamic aeroelastic response of aircraft wings modeled as anisotropic composite thin-walled beams in an incompressible flow and exposed to gust and blast loads is examined. The structural model incorporates a number of nonclassical effects, such as transverse shear, material anisotropy, warping inhibition, and rotatory inertia. The circumferentially asymmetric stiffness layup is used to generate preferred elastic couplings, and in this context, the implication of elastic coupling, warping inhibition on the response is investigated. The unsteady incompressible aerodynamics for arbitrary small motion in the time domain is based on the concept of indicial functions. The implication of directionality property of composite material is revealed, the influence of the gust/blast profiles on the response is discussed, and a number of conclusions are outlined.

Nomenclature

AR	=	wing aspect ratio, L/b
a_{ij}	=	one-dimensional stiffness coefficients
b, d	=	semiwidth and semidepth of the beam cross section, respectively
$C_{L\phi}$	=	local lift curve slope
$F_w, a(s)$	=	primary and secondary warping functions, respectively (see Fig. 3)
G_{sy}	=	effective membrane shear stiffness
$h_{(k)}, h$	=	thickness of the kth layer and thickness of the wall, respectively
K_{ij}	=	reduced stiffness coefficients
L_{ae}	=	unsteady aerodynamic loads
L_g, L_b	=	aerodynamic loads due to gust and blast, respectively
M_F	=	flight Mach number
M_x, M_y	=	one-dimensional stress couples
m	=	number of truncated modes used for the calculation
N	=	number of polynomials used in the shape functions
n	=	number of aerodynamic lag terms used in the approximation of Wagner's function
P_m	=	peak reflected overpressure
$\hat{P}_m$	=	nondimensionalized value of P_m, defined as $bP_m/(2b_1U_n^2)$
Q_z	=	transverse shear force in the z direction
r	=	pulse length factor
U_n	=	chordwise freestream speed, defined as $U_\infty \cos\Lambda$
U_∞	=	streamwise freestream speed
V_G	=	peak gust velocity
w_0, ϕ	=	deflection, rotation about the reference axis
$\hat{w}_0, \hat{\phi}, \hat{\theta}_x$	=	nondimensionalized counterparts of w_0, ϕ, θ_x
$\boldsymbol{X}_{m\times n}$	=	$m \times n$ matrix $\boldsymbol{X}$
$\boldsymbol{X}^T$	=	transpose of the matrix or vector $\boldsymbol{X}$
θ_x	=	rotation of the cross section about x axis
$[\theta_n]$	=	layup scheme
Λ	=	sweep angle
ρ_∞	=	mass density of the freestream
τ	=	nondimensional time variables, defined as $U_n t/b$
τ_p	=	positive phase duration of the pulse
ϕ_W	=	Wagner's function
$\hat{\boldsymbol{\Psi}}_w, \hat{\boldsymbol{\Psi}}_\phi, \hat{\boldsymbol{\Psi}}_x$	=	admissible shape functions vectors with dimension $N \times 1$
ψ_K	=	Küssner's function
ω_{hr}	=	$\sqrt{[a_{33}/(b_1L^4)]}\vert_{\theta=\pi/2}$
$\oint_C, \int_0^L$	=	integral along the cross section and the span, respectively
$\int_{-b}^{b}, \int_{-1}^{1}$	=	airfoil integrals
$[\dot{(\,)}, (\,)']$	=	$[\partial(\,)/\partial t, \partial^2(\,)/\partial^2 t]$
$[\hat{(\,)}, \hat{(\,)}']$	=	$[\partial(\,)/\partial\tau, \partial^2(\,)/\partial\tau^2]$
$[(\,)', (\,)'']$	=	$(\partial(\,)/\partial y, \partial^2(\,)/\partial y^2]$
$[\hat{(\,)}', \hat{(\,)}'']$	=	$[\partial\hat{(\,)}/\partial\eta, \partial^2\hat{(\,)}/\partial\eta^2]$

Received 20 February 2001; revision received 17 May 2002; accepted for publication 20 May 2002.

*Research Associate, Department of Engineering Science and Mechanics.
†Professor, Department of Engineering Science and Mechanics.

I. Introduction

IT is well-known that the next generation of advanced flight vehicles, in general, and combat aircraft of the post-cold era, in particular, are likely to operate in more severe environmental conditions than in the past. In this connection, the dynamic aeroelastic response of advanced aircraft wings to time-dependent external loading, such as gust, sonic boom, and explosive blast-induced loads, is closely related to the level of the operational qualities of these flight vehicles. In spite of the evident practical importance of the problem of determination of the dynamic aeroelastic response of flight vehicles to time-dependent pressure pulses, the specialized literature on this issue is rather scarce. A recent paper[1] considers the problem in a rather comprehensive form, including the combination of various gusts and explosive blast loads. However, the aeroelastic model is still a 2-D one. This paper approaches the problem in an extended context τ, in the sense that the aircraft wing is modeled as an anisotropic thin-walled beam, and based on it, the implications of implementation of the elastic tailoring on the dynamic aeroelastic response are investigated. Special attention is given to the formulation of the problem and the solution methodology. One should remark that due to the nonconservative nature of the problem, the classical modal analysis is not efficient for the solution of the associated eigen/boundary value problem. As pointed out in Ref. 2, the solution of a general nonconservative system requires a state-space description. Correspondingly, the unsteady aerodynamic loads have to be cast into a compatible form, that is, in a finite state form. Other advantages of using a finite state-space form of unsteady aerodynamic loads include that the control can be incorporated very conveniently. In connection with the structural model used in this paper, it should

be stressed that it represents the refined counterpart of the one considered in different contexts in Refs. 3–6. In the sequel, a number of basic ingredients related to the pertinent governing equations will be displayed.

II. Formulation of the Governing System

A. Structural Model

A single-cell, closed cross section, fiber-reinforced composite thin-walled beam is used in the modeling of advanced aircraft wings and toward the study of dynamic subcritical aeroelastic response. Becasue of the importance demonstrated in Refs. 3–11, a number of nonclassical effects have to be considered, which include transverse shear, warping inhibition,[3–6] three-dimensional strain, and contour-wise shear stiffness variation effects[6,7,10,11]. For an overall assessment of these nonclassical effects within the context of composite beams, see Ref. 12. Note that the original development of the beam theory in Refs. 3–5 does not consider the variation of contour-wise shear stiffness, which was later extended in Ref. 6. For the geometric configuration and the chosen coordinate system that is usually adopted in the analyses of aircraft wings, see Figs. 1–3. Based on the basic assumptions stated in Refs. 3–5 and adopted here, the following representation of the three-dimensional displacement quantities is postulated:

$$u(x, y, z, t) = u_0(y, t) + z\phi(y, t) \tag{1a}$$

$$v(x, y, z, t) = v_0(y, t) + \left[x(s) - n\frac{dz}{ds}\right]\theta_z(y, t) + \left[z(s) + n\frac{dx}{ds}\right]\theta_x(y, t) - [F_w(s) + na(s)]\phi'(y, t) \tag{1b}$$

$$w(x, y, z, t) = w_0(y, t) - x\phi(y, t) \tag{1c}$$

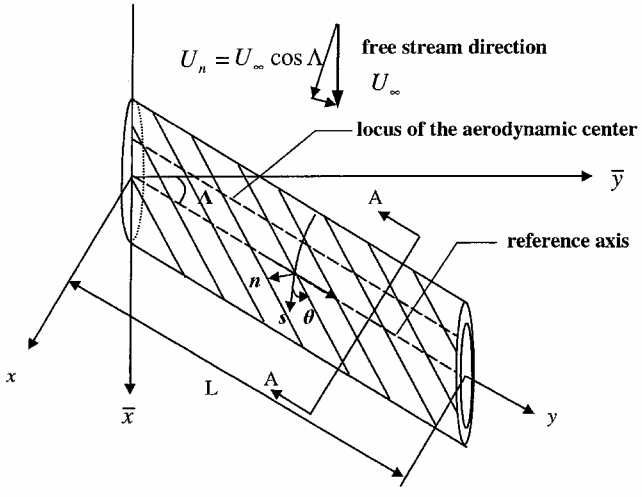

Fig. 1 Geometry of an aircraft wing modeled as thin-walled beam.

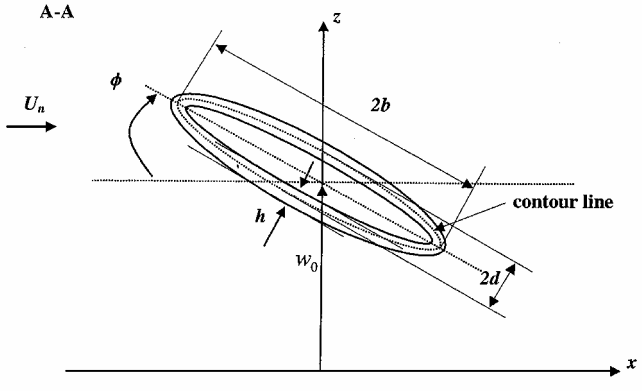

Fig. 2 Geometry of the normal cross section.

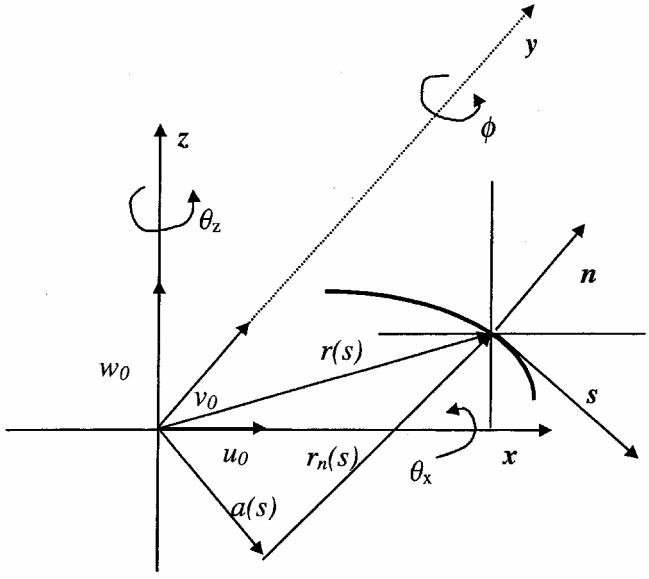

Fig. 3 Displacement field for the beam model.

where

$$\theta_x(y, t) = \gamma_{yz}(y, t) - w_0'(y, t), \qquad \theta_z(y, t) = \gamma_{xy}(y, t) - u_0'(y, t)$$

$$a(s) = -\left(z\frac{dz}{ds} + x\frac{dx}{ds}\right) \tag{2a}$$

In the preceding expressions, $\theta_x(y, t)$, $\theta_z(y, t)$, and $\phi(y, t)$ are the rotations of the cross section about the axes x and z and the twist about the y axis, respectively, whereas $\gamma_{yz}(y, t)$ and $\gamma_{xy}(y, t)$ are the transverse shear strain measures.

The principal warping function in Eq. (1) is expressed as

$$F_w(s) = \int_0^s [r_n(s) - \psi(s)]\,ds \tag{3}$$

in which the torsional function $\psi(s)$ and the quantity $r_n(s)$ are expressed as

$$\psi(s) = \frac{\oint_C r_n(\bar{s})\,d\bar{s}}{h(s)G_{sy}(s)\oint_C [d\bar{s}/h(\bar{s})G_{sy}(\bar{s})]}, \qquad r_n(s) = z\frac{dx}{ds} - x\frac{dz}{ds} \tag{4}$$

where $G_{sy}(s)$ is the effective membrane shear stiffness, which is defined as[6]

$$G_{sy}(s) = \frac{N_{sy}}{h(s)\gamma_{sy}^0(s)} \tag{5}$$

Notice that for the thin-walled beam theory considered herein, the six kinematic variables, $u_0(y, t)$, $v_0(y, t)$, $w_0(y, t)$, $\theta_x(y, t)$, $\theta_z(y, t)$, and $\phi(y, t)$, which represent one-dimensional displacement measures, constitute the basic unknowns of the problem. When the transverse shear effect is discarded, Eq. (2) degenerates to $\theta_x = -w_0'$ and $\theta_z = -u_0'$, and as a result, the number of basic unknown quantities reduces to four. Such a case leads to the classical, unshearable beam model.

The strains contributing to the potential energy are as

Spanwise strain:

$$\varepsilon_{yy}(n, s, y, t) = \varepsilon_{yy}^0(s, y, t) + n\varepsilon_{yy}^1(s, y, t) \tag{6a}$$

where

$$\varepsilon_{yy}^0(s, y, t) = v_0'(y, t) + \theta_z'(y, t)x(y, t) - \phi''(y, t)F_w(s) \tag{6b}$$

$$\varepsilon_{yy}^1(s, y, t) = -\theta_z'(y, t)\frac{dz}{ds} + \theta_x'(y, t)\frac{dx}{ds} - a(s)\phi''(y, t) \tag{6c}$$

are the axial strain components associated with the primary and secondary warping, respectively.

Tangential shear strain:

$$\gamma_{sy}(s, y, t) = \gamma^0_{sy}(s, y, t) + \psi(s)\phi'(y, t) \tag{7a}$$

where

$$\gamma^0_{sy}(s, y, t) = \gamma_{xy}\frac{\mathrm{d}x}{\mathrm{d}s} + \gamma_{yz}\frac{\mathrm{d}z}{\mathrm{d}s} = [u'_0 + \theta_z]\frac{\mathrm{d}x}{\mathrm{d}s} + [w'_0 + \theta_x]\frac{\mathrm{d}z}{\mathrm{d}s} \tag{7b}$$

Transverse shear strain measure:

$$\gamma_{ny}(s, y, t) = -\gamma_{xy}\frac{\mathrm{d}z}{\mathrm{d}s} + \gamma_{yz}\frac{\mathrm{d}x}{\mathrm{d}s} = -[u'_0 + \theta_z]\frac{\mathrm{d}z}{\mathrm{d}s} + [w'_0 + \theta_x]\frac{\mathrm{d}x}{\mathrm{d}s} \tag{8}$$

The stress resultants and stress couples can be reduced to the following expressions:

$$\begin{Bmatrix} N_{yy} \\ N_{sy} \\ L_{yy} \\ L_{sy} \end{Bmatrix} = \begin{bmatrix} K_{11} & K_{12} & K_{13} & K_{14} \\ K_{21} & K_{22} & K_{23} & K_{24} \\ K_{41} & K_{42} & K_{43} & K_{44} \\ K_{51} & K_{52} & K_{53} & K_{54} \end{bmatrix} \begin{Bmatrix} \varepsilon^0_{yy} \\ \gamma^0_{sy} \\ \phi' \\ \varepsilon^1_{yy} \end{Bmatrix} \tag{9a}$$

$$N_{ny} = \left[A_{44} - A^2_{45}/A_{55}\right]\gamma_{ny} \tag{9b}$$

in which the reduced stiffness coefficients K_{ij} are defined in Appendix A.

B. Unsteady Aerodynamic Loads for Arbitrary Small Motion in Incompressible Flow

Based on the strip theory and two-dimensional incompressible unsteady aerodynamics, the unsteady aerodynamic lift and aerodynamic twist moment about the reference axis (the locus of the midchord points is adopted as the reference axis) can be expressed as (Fig. 2)[13]:

$$L_{ae}(y, t) = \rho_\infty U_n \Gamma_0(y, t) - \rho_\infty \frac{\mathrm{d}}{\mathrm{d}t}\int_{-b}^{b} \gamma_0(x, y, t)x\,\mathrm{d}x + \rho_\infty U_n \int_{-b}^{\infty} \frac{\gamma_w(x, y, t)}{\sqrt{x^2 - b^2}}\,\mathrm{d}x \tag{10a}$$

$$T_{ae}(y, t) = -\rho_\infty U_n \int_{-b}^{b} \gamma_0(x, y, t)x\,\mathrm{d}x + \frac{1}{2}\rho_\infty \frac{\mathrm{d}}{\mathrm{d}t}\int_{-b}^{b} \gamma_0(x, y, t)\left(x^2 - \frac{1}{2}b^2\right)\mathrm{d}x + \frac{1}{2}\rho_\infty U_n b^2 \int_{-b}^{\infty} \frac{\gamma_w(x, y, t)}{\sqrt{x^2 - b^2}}\,\mathrm{d}x \tag{10b}$$

where U_n is the freestream speed normal to the leading edge, $\gamma_0(x, y, t)$ is the quasi-steady distributed bound vortex intensity (on the wing), $\gamma_w(x, y, t)$ is the vortex intensity in the wake, and $\Gamma_0(y, t)$ is the quasi-steady circulation. From the potential aerodynamic theory, $\gamma_0(x, y, t)$ and $\gamma_w(x, y, t)$ can be uniquely determined by the boundary (no-penetration) condition and the Kutta condition, as illustrated in the following.

Expressed in the body-fixed frame[14,15] (Fig. 2), the vertical position of the wing cross section can be expressed as

$$z_a(x, y, t) = w_0(y, t) - \phi(y, t)x \tag{11}$$

where $w_0(y, t)$ and $\phi(y, t)$ are the plunging displacement of the points belonging to the reference axis and the twist about this axis, respectively. Note that the rigid angle of attack is not included in this paper.

Denote $F(x, y, z, t) = z_a(x, y, t) - w_0(y, t) - \phi(y, t)x = 0$ as the surface of the wing at time t, then the no-penetration condition of the flow can be expressed as:

$$\frac{\mathrm{D}F(x, y, t)}{\mathrm{D}t} = \frac{\partial F}{\partial t} + \mathbf{U}\cdot\nabla F = \frac{\partial F}{\partial t} + (U_n + u_b + u_w)\frac{\partial F}{\partial x} + v\frac{\partial F}{\partial y} + (w_b + w_w)\frac{\partial F}{\partial z} = 0 \tag{12}$$

where $u_b = \partial\Phi_b/\partial x$, $u_w = \partial\Phi_w/\partial x$, and $w_b = \partial\Phi_b/\partial z$, and $w_w = \partial\Phi_w/\partial z$, in which Φ_b and Φ_w are potential functions of the bound vortex and wake τ, respectively. Based on the thin-airfoil theory and small perturbation assumption,[14] we get

$$w_b(x, y, z, t)|_{z\to 0} = \left.\frac{\partial\Phi_b}{\partial z}\right|_{z\to 0} = -\frac{1}{2\pi}\int_{-b}^{b} \frac{\gamma_b(\xi, y, t)\,\mathrm{d}\xi}{x - \xi} \tag{13a}$$

$$w_w(x, y, z, t)|_{z\to 0} = \left.\frac{\partial\Phi_w}{\partial z}\right|_{z\to 0} = -\frac{1}{2\pi}\int_{b}^{\infty} \frac{\gamma_w(\xi, y, t)\,\mathrm{d}\xi}{x - \xi} \tag{13b}$$

and the downwash

$$w_a(x, y, t) \equiv \frac{\partial z_a}{\partial t} + U_n\frac{\partial z_a}{\partial x} = \dot{w}_0 - x\dot{\phi} - U_n\phi = -\frac{1}{2\pi}\int_{-b}^{b} \frac{\gamma_b(\xi, y, t)\,\mathrm{d}\xi}{x - \xi} - \frac{1}{2\pi}\int_{b}^{\infty} \frac{\gamma_w(\xi, y, t)\,\mathrm{d}\xi}{x - \xi} \tag{13c}$$

In Eqs. (13b) and (13c), the wake is assumed to be in a flat plane. From Eq. (13c), the downwash quantities at the mid- and three-quarter-chord locations are

$$w_{0.5c}(y, t) \equiv w_a(x, y, t)|_{x=0} = \dot{w}_0 - U_n\phi \tag{14a}$$

$$w_{0.75c}(y, t) \equiv w_a(x, y, t)|_{x=\frac{1}{2}b} = \dot{w}_0 - U_n\phi - \tfrac{1}{2}b\dot{\phi} \tag{14b}$$

Following the works by von Kármán and Sears,[13] (Ref. 14 and Theodorsen,[16] the aerodynamic loads can be separated into two parts: the quasi-steady part (solution that ignores the influence of the wake) and the part that corresponds to the influence of the wake. Correspondingly, the bound vortex $\gamma_b(x, y, t)$ can also be separated into two parts, $\gamma_0(x, y, t)$ and $\gamma_1(x, y, t)$.

For the quasi-steady part of the solution,

$$w_a(x, y, t) \equiv \dot{w}_0 - x\dot{\phi} - U_n\phi = -\frac{1}{2\pi}\int_{-b}^{b} \frac{\gamma_0(\xi, y, t)\,\mathrm{d}\xi}{x - \xi} \tag{15a}$$

$$\Gamma_0(y, t) = \int_{-b}^{b} \gamma_0(\xi, y, t)\,\mathrm{d}\xi \tag{15b}$$

whereas for the influence of the wake

$$-\frac{1}{2\pi}\int_{-b}^{b} \frac{\gamma_1(\xi, y, t)\,\mathrm{d}\xi}{x - \xi} - \frac{1}{2\pi}\int_{b}^{\infty} \frac{\gamma_w(\xi, y, t)\,\mathrm{d}\xi}{x - \xi} = 0 \tag{16a}$$

$$\Gamma_1(y, t) = \int_{-b}^{b} \gamma_1(\xi, y, t)\,\mathrm{d}\xi = \int_{b}^{\infty} \left[\sqrt{\frac{\xi + b}{\xi - b}} - 1\right]\gamma_w(\xi, y, t)\,\mathrm{d}\xi \tag{16b}$$

Obviously, the total circulation on the airfoil is

$$\Gamma_b(y, t) = \Gamma_0(y, t) + \Gamma_1(y, t) \tag{17}$$

The Kutta condition applied at the trailing edge is (see Ref. 14)

$$\Gamma_0(y, t) + \int_{b}^{\infty} \sqrt{\frac{\xi + b}{\xi - b}}\gamma_w(\xi, y, t)\,\mathrm{d}\xi = 0 \tag{18}$$

The procedure of the solution consists, first, of solving the integral equation (15a) by using Söhngen's inverse formulas of integral equations (see Ref. 14), then obtaining the expression of $\gamma_0(x, y, t)$ and $\Gamma_0(y, t)$, and solving the integral equation (18) to obtain the expression of $\gamma_w(x, y, t)$. In his paper,[17] Sears has shown that the spatial Laplace transform technique can significantly reduce the complexity of the derivations. Finally, we get

$$\Gamma_0(y,t) = -2b\int_{-1}^{1}\sqrt{\frac{1+\hat{\xi}}{1-\hat{\xi}}}[\dot{w}_0 - U_n\phi - b\hat{\xi}\dot{\phi}]\,\mathrm{d}\hat{\xi} = -2\pi b\left[\dot{w}_0 - U_n\phi - \frac{1}{2}b\dot{\phi}\right] \equiv -2\pi b w_{0.75c}(y,t) \tag{19a}$$

$$L_{ae}(y,t) = -\pi\rho_\infty b^2[\dot{w}_{0.5c}(y,t)] - \underline{2\pi\rho_\infty U_n b\left\{w_{0.75c}(y,0)\phi_W\left(\frac{U_n t}{b}\right) + \int_0^t \frac{\mathrm{d}w_{0.75c}(t_0)}{\mathrm{d}t_0}\phi_W\left[\frac{U_n}{b}(t-t_0)\right]\mathrm{d}t_0\right\}} \tag{19b}$$

$$T_{ae}(y,t) = -\pi\rho_\infty b^3\left[\frac{1}{2}U_n\dot{\phi} + \frac{1}{8}b\ddot{\phi}\right] - \underline{\pi\rho_\infty U_n b^2\left\{w_{0.75c}(y,0)\phi_W\left(\frac{U_n t}{b}\right) + \int_0^t \frac{\mathrm{d}w_{0.75c}(t_0)}{\mathrm{d}t_0}\phi_W\left[\frac{U_n}{b}(t-t_0)\right]\mathrm{d}t_0\right\}} \tag{19c}$$

where ϕ_W is Wagner's function fulfilling

$$\frac{\mathrm{d}\phi_W(\tau)}{\mathrm{d}\tau} + \phi_W(0^+)\delta(\tau) = \mathcal{L}^{-1}\left[\frac{K_1(p)}{K_0(p)+K_1(p)}\right] \tag{20}$$

in which $\tau = U_n t/b$ is the nondimensional time, $\mathcal{L}^{-1}$ the inverse Laplace transform operator, p the Laplace transform variable (the counterpart of τ), and $\delta(\tau)$ the delta Dirac's function, whereas $K_0(p)$ and $K_1(p)$ are the modified Bessel functions of the second kind (see Refs. 2 and 17), and 0^+ denotes that τ approaches 0 from the right side. In Eqs. (19b) and (19c), the underlined terms are associated with the circulatory part of the aerodynamic loads. The quantity $K_1(p)/[K_0(p)+K_1(p)] \equiv C(p)$ is identified as the generalized Theodorsen[16] function in the Laplace transformed space (see Ref. 18).

To cast L_{ae} and T_{ae} into state-space form, the approximate exponential form of Wagner's function is used:

$$\phi_W(\tau) = \left[1.0 - \sum_{i=1}^{n}\alpha_i \exp(-\beta_i\tau)\right]H(\tau) \tag{21}$$

where $H(\tau)$ is the step function.

By denoting

$$\mathrm{D}(y,t) \equiv \int_0^t \frac{\partial w_{0.75c}(y,t_0)}{\partial t_0}\phi_W\left[\frac{U_n(t-t_0)}{b}\right]\mathrm{d}t_0 \tag{22}$$

we get

$$\mathrm{D}(y,t) = w_{0.75c}(y,t) - \sum_{i=1}^{n}\alpha_i B_i(y,t) \tag{23a}$$

where $B_i(y,t)$ satisfies the condition

$$\dot{B}_i + [\beta_i(U_n/b)]B_i = \dot{w}_{0.75c}(y,t) \tag{23b}$$

In the following developments, we assume that the wing starts from rest.

Compared with the methods based on the transfer function realization, the present method can easily model as many as necessary aerodynamic lag terms into the finite state-space form. Note that this method yields the same number of augmented states as those provided by the Roger's approximation method (see Ref. 19).

The preceding results are for two-dimensional cross section wings. For a finite span wing, the modified strip theory[14,20] is used to extend the two-dimensional aerodynamics to three dimensions. First, to be able to approach the case of swept aircraft wings also, the reference coordinate system is being rotated with the wing by the sweep angle Λ (Ref. 14). Second, the lift curve slope 2π and the downwash boundary condition, that is, three-quarter rule for two-dimensional aerodynamics model, are modified to account for the finite span effects[14,20,21]:

$$2\pi \to C_{L\phi} \equiv \frac{\mathrm{d}C_L}{\mathrm{d}\phi} = \frac{AR}{AR + 2\cos\Lambda}2\pi, \qquad \frac{1}{2}b \to b\left[\frac{C_{L\phi}}{2\pi} - \frac{1}{2}\right] \tag{24}$$

Note that only the circulatory terms in Eqs. (19b) and (19c) will be modified.[20,21] All of the geometric measures are now taken in the rotated chordwise coordinate system (Fig. 1a).

For the frame transformation, we follow the procedure in Ref. 14. After collecting the coefficients of the chordwise coordinate x, the downwash in the rotated coordinate system is expressed as:

$$w_a(x,y,t) \cong \frac{\partial z_a}{\partial t} + \frac{\partial z_a}{\partial \bar{x}} = \frac{\partial z_a}{\partial t} + U_\infty\left(\frac{\partial z_a}{\partial x} + \frac{\partial z_a}{\partial y}\sin\Lambda\right)$$

$$= \left[\dot{w}_0 - U_\infty\phi\cos\Lambda + U_\infty\sin\Lambda\frac{\partial w_0}{\partial y}\right]$$

$$-x\left[\dot{\phi} + U_\infty\frac{\partial\phi}{\partial y}\sin\Lambda\right] \tag{25}$$

Replacing $\dot{w}_0 - U_n\phi$ by $\dot{w}_0 - U_\infty\phi\cos\Lambda + U_\infty\sin\Lambda(\partial w_0/\partial y)$ and $\dot{\phi}$ by $\dot{\phi} + U_\infty(\partial\phi/\partial y)\sin\Lambda$ in the preceding formulas, and denoting $U_n \equiv U_\infty\cos\Lambda$, we get

$$w_{0.75c}(y,t) = \dot{w}_0 - U_n\phi + U_n\tan\Lambda\frac{\partial w_0}{\partial y}$$

$$-\frac{b}{2}\left[\dot{\phi} + U_n\frac{\partial\phi}{\partial y}\tan\Lambda\right]\left[\frac{C_{L\phi}}{\pi} - 1\right] \tag{26a}$$

$$w_{0.5c}(y,t) = \dot{w}_0 - U_n\phi + U_n\tan\Lambda\frac{\partial w_0}{\partial y} \tag{26b}$$

Based on these equations, the explicit expressions of unsteady aerodynamic lift and moment will be given in the following sections.

C. Gust and Blast Loads

Based on Duhamel's convolution integral and the indicial function for an arbitrary gust $w_G(\tau)$, the induced aerodynamic lift is expressed as

$$L_g(\tau) = C_{L\phi}bU_n\left[w_G(0)\psi_K(\tau) + \int_0^\tau \frac{\partial w_G(\tau_0)}{\partial\tau_0}\psi_K(\tau-\tau_0)\,\mathrm{d}\tau_0\right] \tag{27}$$

where

$$\psi_K(\tau) = \mathcal{L}^{-1}\left((1/pe^p)\{1/[K_0(p)+K_1(p)]\}\right)$$

is the Küssner's function (see Ref. 16). In the practical calculation, ψ_K can be approximated by the following exponential form[14]:

$$\psi_K(\tau) = 1 - 0.500e^{-0.130\tau} - 0.500e^{-1.00\tau}, \qquad \tau > 0 \tag{28}$$

As proved by von Kármán and Sears,[13] the gust embedded in the atmosphere and flowing with the atmosphere always acts at the quarter-chord position, even when the aerodynamic load is not completely circulatory. For simplicity, we assume that the gust is not affected by the penetration of the wing. Therefore, the aerodynamic moment about the reference axis due to the gust is

$$T_g(\tau) = \frac{1}{2}bL_g(\tau) = \frac{1}{2}C_{L\phi}b^2U_n\left[w_G(0)\psi_K(\tau) + \int_0^\tau \frac{\partial w_G(\tau_0)}{\partial \tau_0}\psi_K(\tau-\tau_0)\,\mathrm{d}\tau_0\right] \tag{29}$$

In general, a gust (discrete model, as considered in this paper) can be specified by the gust intensity, gradient and its profile.[14] In this paper, the gust intensity is assumed to be uniformly distributed along the span. The following types of gust are used in the present study of aeroelastic response.

Sharp-edged gust:

$$w_G(\tau) = H(\tau)V_G$$

1-COSINE gust:

$$w_G(\tau) = \tfrac{1}{2}V_G[1-\cos(\pi\tau/\tau_p)][H(\tau) - H(\tau - 2\tau_p)]$$

where V_G is the peak gust velocity and τ_p is the gust gradient expressed in semichord length.[12] Other types of gusts are listed in Ref. 1.

The blast load due to a sonic boom signature can be modeled as an N-shaped pressure pulse[1,7]

$$L_b(\tau) = P_m(1-\tau/\tau_p)[H(\tau) - H(\tau - r\tau_p)] \tag{30}$$

in which P_m is the peak reflected pressure in excess of the ambient pressure, τ_p is the positive phase duration of the pressure pulse, and r is the pulse length factor.[1,7] When $r=1$, the N-shaped pulse degenerates into an explosive pulse (in triangular form), whereas when $r=2$, a symmetric sonic-boom pulse is obtained.[1] For blast loads, we assume that these act throughout the wing.

D. Governing System

The governing equations and boundary conditions can be systematically derived from the extended Hamilton's principle (see Ref. 2), which states that the true path of motion renders the following variational form stationary:

$$\int_{t_1}^{t_2}(\delta T - \delta V + \overline{\delta W_e})\,\mathrm{d}t = 0 \tag{31a}$$

with

$$\delta u_0 = \delta v_0 = \delta w_0 = \delta\theta_x = \delta\theta_z = \delta\phi = 0 \quad \text{at} \quad t = t_1,\ t_2 \tag{31b}$$

where T and V are the kinetic and the strain energy, respectively, whereas $\overline{\delta W_e}$ is the virtual work due to external forces. These are defined as

Kinetic energy:

$$T = \frac{1}{2}\int_0^L \oint_C \sum_{k=1}^{m_l}\int_{h_{(k)}} \rho_{(k)}\left[\left(\frac{\partial u}{\partial t}\right)^2 + \left(\frac{\partial w}{\partial t}\right)^2 + \left(\frac{\partial v}{\partial t}\right)^2\right]\mathrm{d}n\,\mathrm{d}s\,\mathrm{d}y \tag{32}$$

Strain energy:

$$V = \frac{1}{2}\int_\tau \sigma_{ij}\varepsilon_{ij}\,\mathrm{d}\tau = \frac{1}{2}\int_0^L \oint_C \sum_{k=1}^{m_l}\int_{h_{(k)}} [\sigma_{yy}\varepsilon_{yy} + \sigma_{sy}\gamma_{sy} + \sigma_{ny}\gamma_{ny}]_{h_{(k)}}\,\mathrm{d}n\,\mathrm{d}s\,\mathrm{d}y \tag{33}$$

Virtual work due to unsteady aerodynamic, gust, and blast loads:

$$\overline{\delta W_e} = \int_0^L [p_z(y,t)\delta w_0(y,t) + m_y(y,t)\delta\phi(y,t)]\,\mathrm{d}y \tag{34}$$

where $p_z = L_{ae} + L_g + L_b$ (positive upward) is the combined aerodynamic force per unit span length and $m_y = T_{ae} + T_g$ (positive nose-up) are aerodynamic twist moments about the reference axis.

To study the dynamic aeroelastic response, an aircraft wing featuring a biconvex cross section and experiencing bending–twist coupling is considered. To this end, the circumferentially asymmetric stiffness (CAS) layup[9] is adopted. As demonstrated in Refs. 4 and 5, this type of beam features the following two sets of independent elastic couplings: 1) vertical bending/twist/vertical transverse shear (w_0, ϕ, θ_x) and 2) extension/lateral bending/lateral transverse shear (u_0, v_0, θ_z). Also, the aerodynamic loads and the inertia forces of the beams are completely split into these above two groups; hence, the total equations of motion and the boundary conditions are completely decoupled. The equations of motion of the first group that are of interest for the present problem are

$$\delta w_0:\ Q_z' + L_{ae} + L_g + L_b - b_1\ddot{w}_0 = 0 \tag{35a}$$

$$\delta\phi:\ M_y' - B_w'' + T_{ae} + T_g - (b_4+b_5)\ddot{\phi} + (b_{10}+b_{18})\ddot{\phi}'' = 0 \tag{35b}$$

$$\delta\theta_x:\ M_x' - Q_z - (b_4+b_{14})\ddot{\theta}_x = 0 \tag{35c}$$

The boundary conditions are, at $y=0$,

$$w_0 = 0, \qquad \phi = 0, \qquad \phi' = 0, \qquad \theta_x = 0 \tag{36a}$$

and at $y=L$,

$$Q_z = 0, \qquad -B_w' + M_y + (b_{10}+b_{18})\ddot{\phi}' = 0$$
$$B_w = 0, \qquad M_x = 0 \tag{36b}$$

In the preceding equations, M_x, Q_z, B_w, and M_y are the one-dimensional stress resultant and stress couple measures that are defined as

$$M_x(y,t) = \oint_C \left(zN_{yy} + L_{yy}\frac{\mathrm{d}x}{\mathrm{d}s}\right)\mathrm{d}s$$

$$Q_z(y,t) = \oint_C \left(N_{sy}\frac{\mathrm{d}z}{\mathrm{d}s} + N_{ny}\frac{\mathrm{d}x}{\mathrm{d}s}\right)\mathrm{d}s$$

$$B_w(y,t) = -\oint_C [F_w(s)N_{yy} + a(s)L_{yy}]\,\mathrm{d}s$$

$$M_y(y,t) = \oint_C N_{sy}\psi(s)\,\mathrm{d}s \tag{37}$$

The inertia coefficients b_1, b_4, b_5, b_{10}, b_{14}, b_{15}, and b_{18} are defined in Appendix A.

For biconvex cross section thin-walled beams with CAS layup configuration, the force-displacement relations are

$$\begin{Bmatrix} M_x \\ Q_z \\ B_w \\ M_y \end{Bmatrix} = \begin{bmatrix} a_{33} & 0 & 0 & a_{37} \\ 0 & a_{55} & a_{56} & 0 \\ 0 & a_{56} & a_{66} & 0 \\ a_{37} & 0 & 0 & a_{77} \end{bmatrix} \begin{Bmatrix} \theta_x' \\ (w_0' + \theta_x) \\ \phi'' \\ \phi' \end{Bmatrix} \tag{38}$$

For the free warping model,[4,5,8] the force-displacement relations are

$$\begin{Bmatrix} M_x \\ Q_z \\ B_w \\ M_y \end{Bmatrix} = \begin{bmatrix} a_{33} & 0 & a_{37} \\ 0 & a_{55} & 0 \\ 0 & a_{56} & 0 \\ a_{37} & 0 & a_{77} \end{bmatrix} \begin{Bmatrix} \theta_x' \\ (w_0' + \theta_x) \\ \phi' \end{Bmatrix} \tag{39}$$

In terms of the basic unknowns, the governing equations that include all of the mentioned effects are

$$\delta w_0 : a_{55}(w_0'' + \theta_x') + \underline{\underline{a_{56}\phi'''}} + L_{ae} + L_g + L_b - b_1\ddot{w}_0 = 0 \quad (40a)$$

$$\delta\phi : a_{37}\theta_x'' + a_{77}\phi'' - a_{56}(w_0''' + \theta_x'') - \underline{\underline{a_{66}\phi^{(IV)}}} + T_{ae} + T_g - (b_4 + b_5)\ddot{\phi} + \underline{\underline{(b_{10} + b_{18})\ddot{\phi}''}} = 0 \quad (40b)$$

$$\delta\theta_x : a_{33}\theta_x'' + a_{37}\phi'' - a_{55}(w_0' + \theta_x) - \underline{\underline{a_{56}\phi''}} - \underline{(b_4 + b_{14})\ddot{\theta}_x} = 0 \quad (40c)$$

The boundary conditions are, at $y = 0$

$$w_0 = 0, \qquad \phi = 0, \qquad \underline{\underline{\phi' = 0}}, \qquad \theta_x = 0 \quad (41a\text{–}d)$$

and at $y = L$ are

$$\delta w_0 : a_{55}(w_0' + \theta_x) + \underline{\underline{a_{56}\phi''}} = 0$$

$$\delta\phi : -a_{56}(w_0'' + \theta_x') - \underline{\underline{a_{66}\phi'''}} + a_{37}\theta_x' + a_{77}\phi' = -(b_{10} + b_{18})\ddot{\phi}'$$

$$\delta\phi' : -a_{56}(w_0' + \theta_x) - \underline{\underline{a_{66}\phi''}} = 0$$

$$\delta\theta_x : a_{33}\theta_x' + a_{37}\phi' = 0 \quad (41e\text{–}f)$$

In Eqs. (40–41) the terms underscored by double solid lines are associated with the warping inhibition effect, whereas the term underscored by single solid line identifies the rotatory inertia effect.[3–5]

The unsteady aerodynamic lift and twist moment are expressed as

$$L_{ae}(y,t) = -\pi\rho_\infty b^2[\dot{w}_{0.5c}(y,t)] - C_{L\phi}\rho_\infty U_n b\left[w_{0.75c}(y,t) - \sum_{i=1}^{n}\alpha_i B_i\right] = -\pi\rho_\infty b^2\left[\ddot{w}_0 + U_n\frac{\partial^2 w_0}{\partial y\partial t}\tan\Lambda - U_n\dot{\phi}\right] - C_{L\phi}\rho_\infty U_n b\left[\dot{w}_0 - U_n\phi + U_n\frac{\partial w_0}{\partial y}\tan\Lambda - \frac{b}{2}\left(\frac{C_{L\phi}}{\pi} - 1\right)\left(\dot{\phi} + U_n\frac{\partial\phi}{\partial y}\tan\Lambda\right) - \sum_{i=1}^{n}\alpha_i B_i\right] \quad (42a)$$

$$T_{ae}(y,t) = -\pi\rho_\infty b^3\left[\frac{1}{2}U_n\dot{\phi} + \frac{1}{8}b\ddot{\phi}\right] - \frac{1}{2}C_{L\phi}\rho_\infty U_n b^2\left[w_{0.75c}(y,t) - \sum_{i=1}^{n}\alpha_i B_i\right] = -\pi\rho_\infty b^3\left\{\left[\frac{1}{2}\left(\frac{C_{L\phi}}{\pi} - 1\right)\left(U_n\dot{\phi} + U_n^2\frac{\partial\phi}{\partial y}\tan\Lambda\right)\right] + \frac{1}{8}b\left[\ddot{\phi} + U_n\frac{\partial^2\phi}{\partial y\partial t}\tan\Lambda\right]\right\} - \frac{1}{2}C_{L\phi}\rho_\infty U_n b^2\left\{\dot{w}_0 - U_n\phi + U_n\frac{\partial w_0}{\partial y}\tan\Lambda - \frac{b}{2}\left(\frac{C_{L\phi}}{\pi} - 1\right)\left(\dot{\phi} + U_n\frac{\partial\phi}{\partial y}\tan\Lambda\right) - \sum_{i=1}^{n}\alpha_i B_i\right\} \quad (42b)$$

In Eqs. (42a), and (42b), B_i fulfill Eq. (23b). The expressions of the gust and blast loads have been provided in Eqs. (27), (29), and (30).

III. Solution Methodology

Because of the nonconservative nature of the boundary value/eigenvalue problems and the high complexity arising from the anisotropy of the constituent materials and the boundary conditions, we apply the nondimensionalization, spatial semidiscretization and then cast the governing equations into state-space form. The spatial semidiscretization is based on the extended Galerkin's method (see Refs. 7 and 22). The conversion of governing equations into state-space form is prompted by the fact that, for a general nonconservative system, the solution requires a state-space description[2] and that the classical modal analysis based on complex eigensystem does not yield an efficient solution. In addition, to treat various gust and blast loads in a unified way, the temporal discretization is implemented. Note that the Laplace transform method (LTM) can only be efficiently applied to sufficiently low-order systems. For the problem being addressed here, this methodology does not constitute the most appropriate one.

A. State-Space Form of the Governing Equations

Define the basic nondimensional parameters:

$$\eta \equiv \frac{y}{L}, \qquad \tau \equiv \frac{U_n t}{b}, \qquad \mathrm{AR} \equiv \frac{L}{b}, \qquad \hat{w}_0(\eta,\tau) \equiv \frac{w_0}{2b}$$

$$\hat{\phi}(\eta,\tau) \equiv \phi(\eta,\tau), \qquad \hat{\theta}_x(\eta,\tau) \equiv \theta_x(\eta,\tau), \qquad \frac{\mathrm{d}(\,)}{\mathrm{d}\tau} = \frac{b}{U_n}\frac{\mathrm{d}(\,)}{\mathrm{d}t} \quad (43)$$

and carry-out spatial semidiscretization:

$$\hat{w}_0(\eta,\tau) = \hat{\boldsymbol{\Psi}}_w^T(\eta)\hat{\boldsymbol{q}}_w(\tau), \qquad \hat{\phi}(\eta,\tau) = \hat{\boldsymbol{\Psi}}_\phi^T(\eta)\hat{\boldsymbol{q}}_\phi(\tau)$$

$$\hat{\theta}_x(\eta,\tau) = \hat{\boldsymbol{\Psi}}_x^T(\eta)\hat{\boldsymbol{q}}_x(\tau) \quad (44a)$$

where the shape functions $\hat{\boldsymbol{\Psi}}_w(\eta)$, $\hat{\boldsymbol{\Psi}}_\phi(\eta)$, and $\hat{\boldsymbol{\Psi}}_x(\eta)$ are only required to fulfill the geometric boundary conditions. In Eq. (44a), $\hat{q}_w(\tau)$, $\hat{q}_\phi(\tau)$ and $\hat{q}_x(\tau)$ are $N \times 1$ generalized displacement vectors, which, by the modal expansion theorem (Ref. 2, pp. 171–178), can be further expressed as:

$$\hat{q}_w(\tau) = \Theta_w\hat{\xi}_s(\tau), \qquad \hat{q}_\phi(\tau) = \Theta_\phi\hat{\xi}_s(\tau), \qquad \hat{q}_x(\tau) = \Theta_x\hat{\xi}_s(\tau) \quad (44b)$$

where, Θ_w, Θ_ϕ, and Θ_x are $N \times m$ matrices consisting of the first m eigenmodes, $\hat{\xi}_s$ are the modal coordinates (Ref. 2, p. 199). After casting the governing equations into state space, we get:

$$\begin{Bmatrix}\dot{\hat{\boldsymbol{x}}}_s\\ \dot{\hat{\boldsymbol{x}}}_a\end{Bmatrix} = \begin{bmatrix}\boldsymbol{A}_s & \boldsymbol{B}_s\\ \boldsymbol{B}_a\boldsymbol{A}_s & \boldsymbol{A}_a + \boldsymbol{B}_a\boldsymbol{B}_s\end{bmatrix}\begin{Bmatrix}\hat{\boldsymbol{x}}_s\\ \hat{\boldsymbol{x}}_a\end{Bmatrix} + \begin{bmatrix}\boldsymbol{0}_{m\times 1}\\ \bar{\boldsymbol{M}}_n^{-1}\\ \boldsymbol{D}_2\bar{\boldsymbol{M}}_n^{-1}\\ \vdots\\ \boldsymbol{D}_2\bar{\boldsymbol{M}}_n^{-1}\end{bmatrix}\{\boldsymbol{Q}_g + \boldsymbol{Q}_b\} \quad (45)$$

or, in a more compact form,

$$\{\dot{\hat{\boldsymbol{X}}}\} = [\boldsymbol{A}]\{\hat{\boldsymbol{X}}\} + [\boldsymbol{B}_e]\{\boldsymbol{Q}_g\} + [\boldsymbol{B}_e]\{\boldsymbol{Q}_b\} \quad (46)$$

In Eq. (45), $\hat{\boldsymbol{x}}_s$ and $\hat{\boldsymbol{x}}_a$ are $2m \times 1$, and $nm \times 1$ vectors that describe the motion of the wing and unsteady aerodynamic loads on the wing, respectively, whereas $\boldsymbol{Q}_g$ and $\boldsymbol{Q}_b$ are the generalized gust and blast loads, respectively. The details of the matrices and vectors in Eq. (46) are listed in Appendix B.

B. Temporal Discretization of the Governing Equations

The general solution of Eq. (46) can be expressed as[2]

$$\{\hat{\boldsymbol{X}}(\tau)\} = [e^{A\tau}]\{\hat{\boldsymbol{X}}(0)\} + \int_0^\tau \{\exp[\boldsymbol{A}(\tau - \tau_0)]\}[\boldsymbol{B}_e]\{\boldsymbol{Q}_g\}(\tau_0) + \{\boldsymbol{Q}_b(\tau_0)\}\,\mathrm{d}\tau_0 \quad (47a)$$

where the transition matrix

$$[e^{A\tau}] = \mathcal{L}^{-1}[(p\boldsymbol{I} - \boldsymbol{A})^{-1}] = \sum_{i=0}^{\infty}\frac{\boldsymbol{A}^i}{i!\tau^i} \quad (47b)$$

For a general nonconservative system, the eigenvalues and eigenvectors are complex-valued quantities. Although the system matrix $\boldsymbol{A}$ can be orthogonalized in terms of its left and right eigenvectors,[2] for large order of $\boldsymbol{A}$ the actual implementation is not efficient.[2] Moreover, the LTM is almost impractical for systems featuring large orders. As a results, the preceding equation is directly discretized in the time domain.

With the fixed sampling step $\Delta\tau$, the following discretized equation is derived[2]:

$$\{\hat{\boldsymbol{X}}(k+1)\} \cong [e^{A\Delta\tau}]\{\hat{\boldsymbol{X}}(k)\} + [\boldsymbol{A}]^{-1}[e^{A\Delta\tau} - \boldsymbol{I}][\boldsymbol{B}_e]\{\boldsymbol{Q}_g(k) + \boldsymbol{Q}_b(k)\} \tag{48a}$$

where the discretized transition matrix

$$[e^{A\Delta\tau}] = \sum_{i=0}^{\infty} \frac{\boldsymbol{A}^i}{i!}(\Delta\tau)^i \tag{48b}$$

Note that, if the external load $\boldsymbol{Q}_g(k) + \boldsymbol{Q}_b(k)$ is constant for all k and $e^{A\Delta\tau}$ is precisely evaluated, then the approximation in Eq. (48) strictly becomes an equality. Given the maximum amplitude of the eigenvalues of $\boldsymbol{A}$ and the sampling step $\Delta\tau$, the numerical convergence requirement of Eq. (48b) and the prescribed computation accuracy determines the number of truncated terms in Eq. (48b) for the approximation of $e^{A\Delta\tau}$ (Ref. 2). In this paper, the accuracy order of 10^{-5} is prescribed.

Once the solution of $\{\hat{\boldsymbol{X}}(k)\}$ is known, the generalized coordinate $\hat{\xi}_s(k)$ can be extracted, and then the aeroelastic response can be reconstructed as follows:

$$\hat{w}_0(\eta,k) = \hat{\boldsymbol{\Psi}}_w^T(\eta)\boldsymbol{\Theta}_w\hat{\xi}_s(k), \qquad \hat{\phi}(\eta,k) = \hat{\boldsymbol{\Psi}}_\phi^T(\eta)\boldsymbol{\Theta}_\phi\hat{\xi}_s(k)$$
$$\hat{\theta}_x(\eta,k) = \hat{\boldsymbol{\Psi}}_x^T(\eta)\boldsymbol{\Theta}_x\hat{\xi}_s(k) \tag{49}$$

For the acceleration, substituting the solution of $\hat{\boldsymbol{X}}(k)$ to Eq. (46) and extracting $\hat{\xi}_s(k)$, we get:

$$\ddot{\hat{w}}_0(\eta,k) = \hat{\boldsymbol{\Psi}}_w^T(\eta)\boldsymbol{\Theta}_w\ddot{\hat{\boldsymbol{\xi}}}_s(k), \qquad \ddot{\hat{\phi}}(\eta,k) = \hat{\boldsymbol{\Psi}}_\phi^T(\eta)\boldsymbol{\Theta}_\phi\ddot{\hat{\xi}}_s(k)$$
$$\ddot{\hat{\theta}}_x(\eta,k) = \hat{\boldsymbol{\Psi}}_x^T(\eta)\boldsymbol{\Theta}_x\ddot{\hat{\xi}}_s(k) \tag{50}$$

IV. Validation and Discussion

In this section, the dynamic aeroelastic response of anisotropic thin-walled beams exposed to selected gust and blast loads is addressed. Also addressed is the influence of elastic coupling and warping inhibition on the response. The geometric and material specifications of beams with CAS layup are listed in Table 1. Note that in the actual calculation, the first five structural modes and two aerodynamic lag terms [see Eq. (21)] are used, that is, $m = 5$ and $n = 2$, Wagner's function is approximated by the Jones's quasi-polynomial formulas (see Ref. 14), and all of the response components (bending, twist, sand transverse) are measured at the beam tip ($\eta = 1$).

Table 1 Material properties and geometric specifications of a wing with CAS layup and biconvex cross section

Specification	Value
Material	
E_{11}	206.8×10^9 N/m^2
$E_{22} = E_{33}$	5.17×10^9 N/m^2
$G_{13} = G_{23}$	2.55×10^9 N/m^2
G_{12}	3.10×10^9 N/m^2
$\mu_{12} = \mu_{13} = \mu_{23}$	0.25
ρ	1.528×10^3 kg/m^3
Geometric	
Length L	2.032 m
Width $2b$[a]	0.254 m
Depth $2d$[a]	0.06807 m
Aspect ratio	16
Wall thickness h	0.0102 m
Number of layers	6
Layer thickness	0.0017 m
Sweep angle Λ	0 deg

[a]Length is measured on the contour line.

Table 2 Comparison of the flutter results of the Goland's wing[23]

Method	Flutter speed, km/hr	Error,[a] %	Flutter frequency, Hz	Error,[a] %
Exact[23]	494.1	——	11.25	——
Present ($N = 9$)	494.5	0.08	11.04	−1.87
Patil and Hodges[24]	488.3	−1.17	11.17	−0.71
Gern and Librescu[25] ($N = 7$)	493.6	−0.10	12.02	6.84

[a]Relative error, {[approximated] − [exact]}/[exact].

Before addressing these issues, it is in order to validate the accuracy of the aeroelastic model developed so far. Toward this purpose, the flutter prediction of the Goland's wing[23] via the transient method, which is based on Eq. (46), is compared with the exact solution. The comparison predictions, listed in Table 2 (Refs. 23–25), reveal the excellent agreement with the exact ones. Note that the accuracy of the structural model has been validated in Refs. 26 and 27 against available experimental and theoretical results.

Figures 4 and 5 quantitatively display the significant influence of elastic coupling on the response. By choosing the stacking sequences to be $[75_6]$ and $[105_6]$, we retain the stiffnesses a_{33}, a_{77}, a_{55}, and a_{66} to be equal for these two stacking sequences in the sense that they are symmetric with respect to $\theta = 90$ deg, whereas a_{37} and a_{56} are antisymmetric (Fig. 6). It is readily seen that, for the case of $[105_6]$, the maximum amplitudes of both the deflection and twist are reduced to half of their counterparts obtained in the case of $[75_6]$. Note that the damping is entirely due to the unsteady aerodynamic loads (fluid–structure interaction); no structure-related damping is accounted for. One interesting phenomenon about this type of damping is that, although in the $[105_6]$ case the amplitudes of the response are reduced, the damping (or decaying rate) is larger than its counterpart in the case of $[75_6]$. It seems that we can not achieve, simultaneously, reduction in both the amplitude and damping.

The amplitude reduction of the aeroelastic response due to elastic coupling can be viewed as consisting of two sources, one that is entirely due to the structural modification and another one that is due to the fluid–wing interaction (of feedback mechanism). It is noted that the unsteady aerodynamic loads are discarded toward evaluating the structural contribution. Comparison of Figs. 7 and 8 clearly reveals each of these two contributions: In the total change of 0.026, only 0.009 is of structural nature, whereas the remaining 0.017 is due to the fluid–wing interaction. Stated another way, if elastic coupling can achieve one unit of structural modification, almost two more units of modification can be induced further by the fluid–wing interaction. This reveals that fluid–wing interaction significantly amplifies the structural modification due to elastic coupling by a factor of 2. However, the modification of aerodynamic damping does not follow this direction.

Figure 9 shows the influence of warping inhibition effect on the deflection response in cases of large aspect ratio wings. It is readily seen that warping inhibition increases the transverse bending stiffness and, therefore, reduces the response amplitude and shifts the oscillatory frequencies to be higher. However, these modifications are marginal, even in the presence of the amplifying effect by the fluid–wing interaction. This implies that, for wings with large aspect ratio, warping inhibition may be discarded in the analysis of aeroelastic response.

Figure 10 shows the sensitivity of response due to change of τ_p in the one-cosine gust excitation. Observe that the maximum amplitude changes mildly due to these different 1-COSINE gusts. However, for blast or sonic boom, the picture becomes quite different, as shown in Figs. 11 and 12. Observe that the sonic boom ($r = 2$) causes the most severe response.

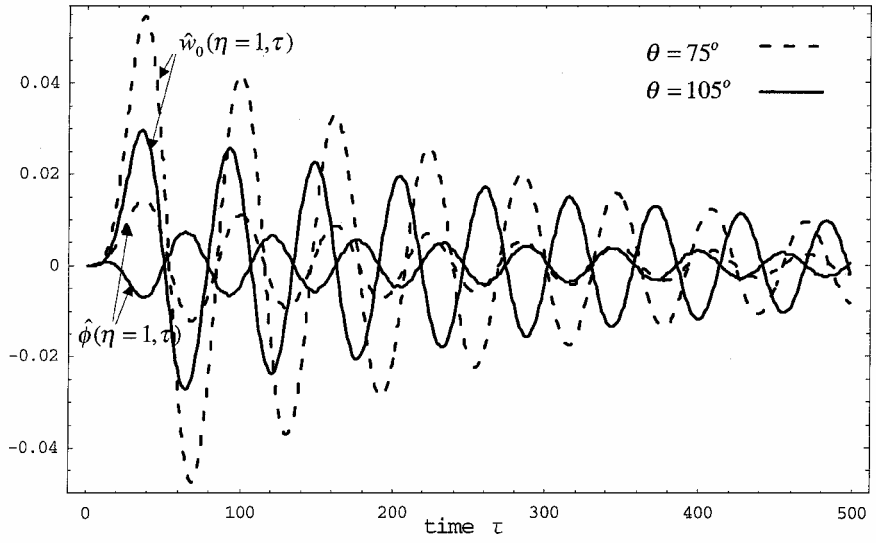

Fig. 4 Influence of elastic coupling on the response subjected to a 1-COSINE gust AR = 16, $M_F = 0.5$, $V_G = 10$ m/s, $\tau_p = 20$, and warping inhibition included.

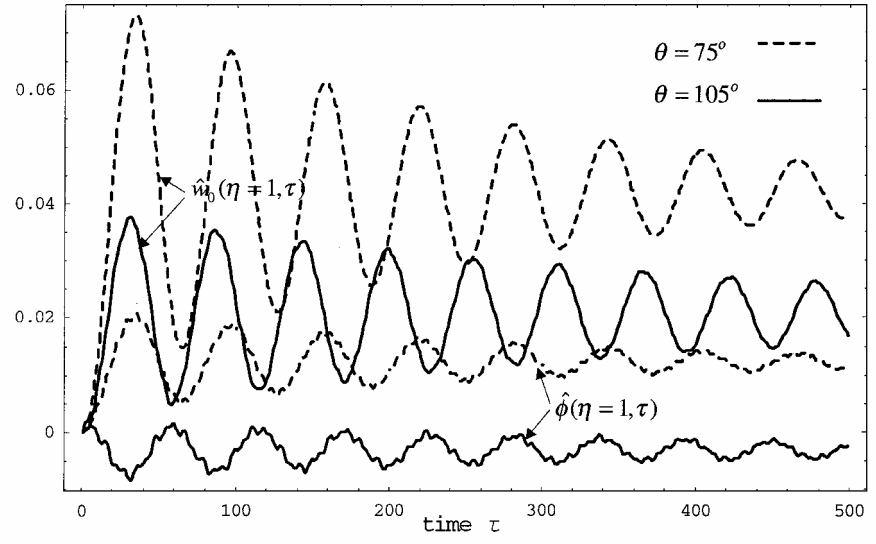

Fig. 5 Influence of elastic coupling on the response subjected to a sharp-edged gust, AR = 16, $M_F = 0.5$, $V_G = 10$ m/s, and warping inhibition included.

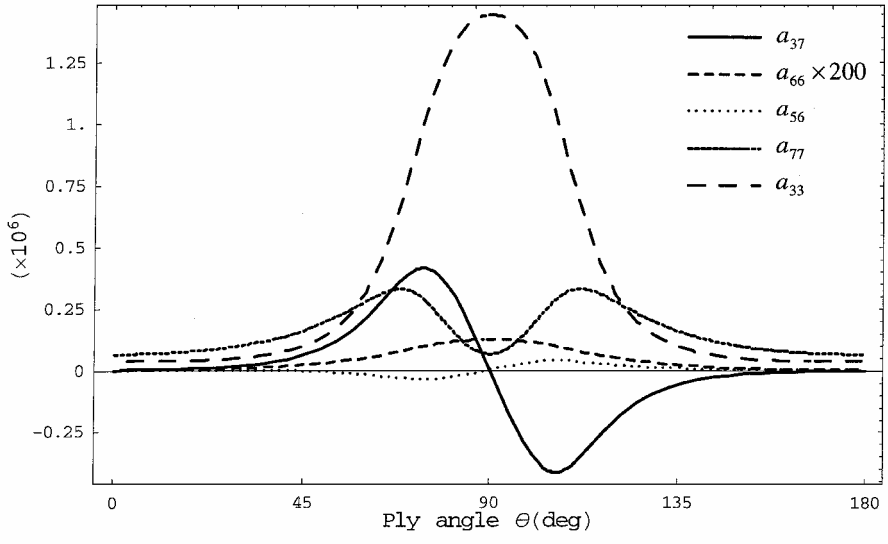

Fig. 6 One-dimensional stiffness coefficients vs ply angle; units: a_{37} (N · m^2), a_{66} (N · m^4), a_{56} (N · m^2), a_{77} (N · m^2), a_{33} (N · m^2), and a_{55} (N).

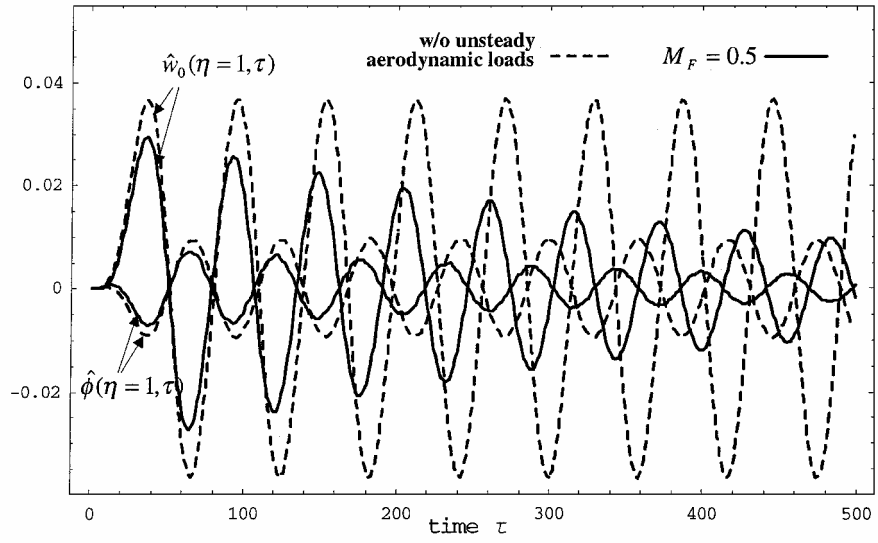

Fig. 7 Influence of fluid–wing interaction on the response subjected to a 1-COSINE gust, [105$_6$], AR = 16, V_G = 10 m/s, τ_p = 20, and warping inhibition included.

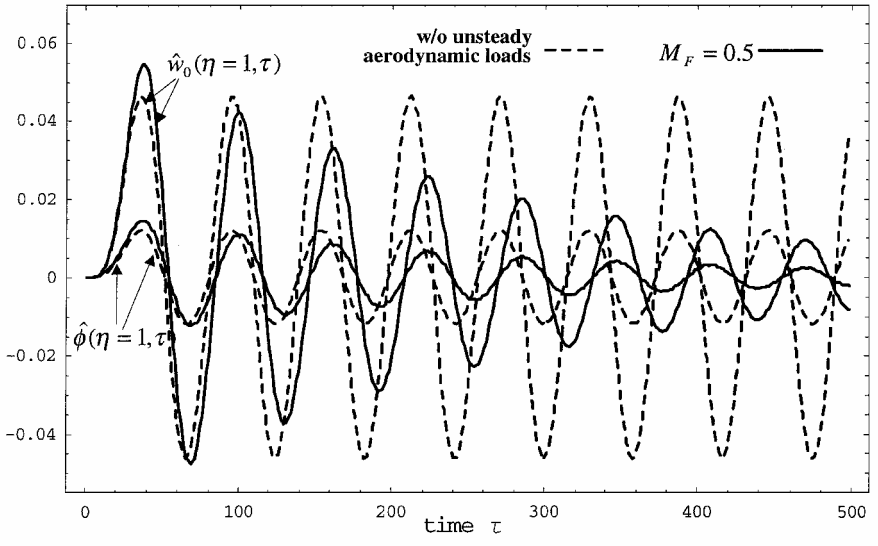

Fig. 8 Influence of fluid–wing interaction on the response subjected to a 1-COSINE gust, [75$_6$], AR = 16, V_G = 10 m/s, τ_p = 20, M_F = 0.5, and warping inhibition included.

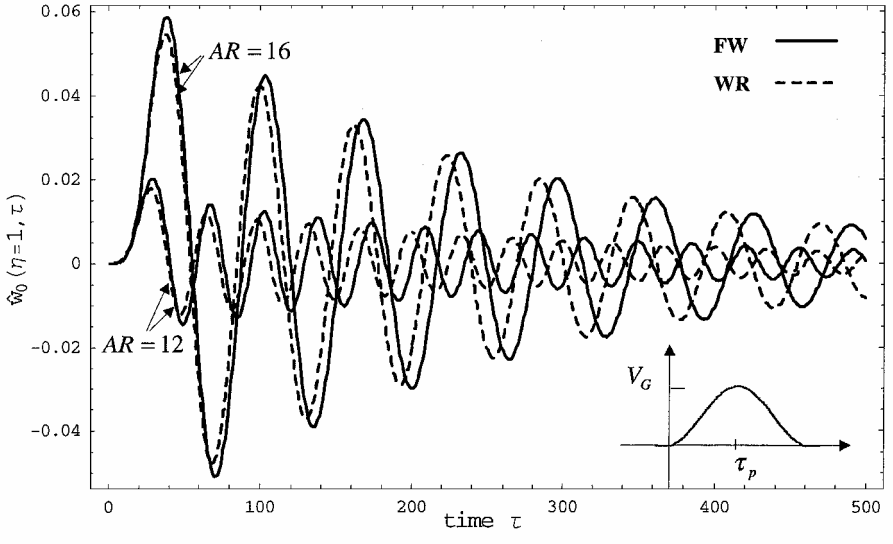

Fig. 9 Warping inhibition effect on the deflection response subjected to a 1-COSINE gust, [75$_6$], V_G = 10 m/s, τ_p = 20, and M_F = 0.5.

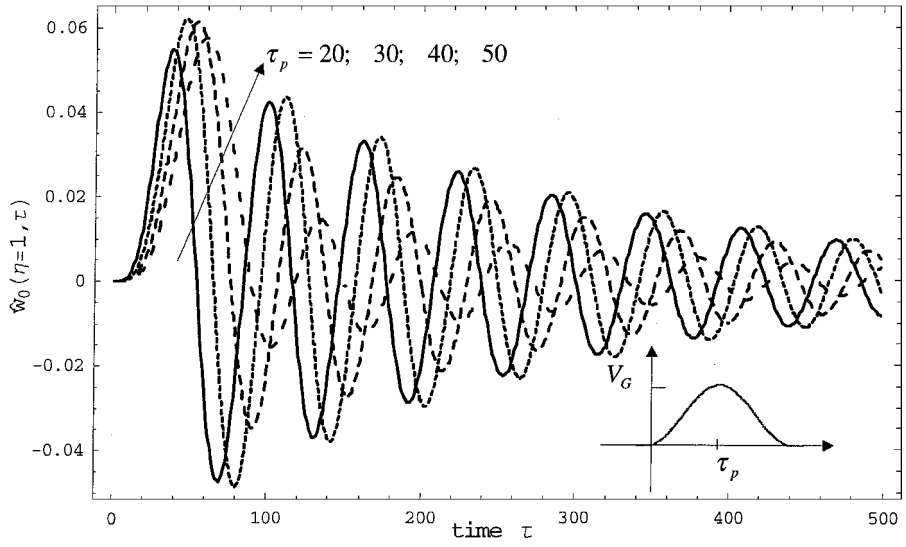

Fig. 10 Response subjected to 1-COSINE gusts with different τ_p, [75$_6$], AR = 16, V_G = 10 m/s, M_F = 0.5, and warping inhibition included.

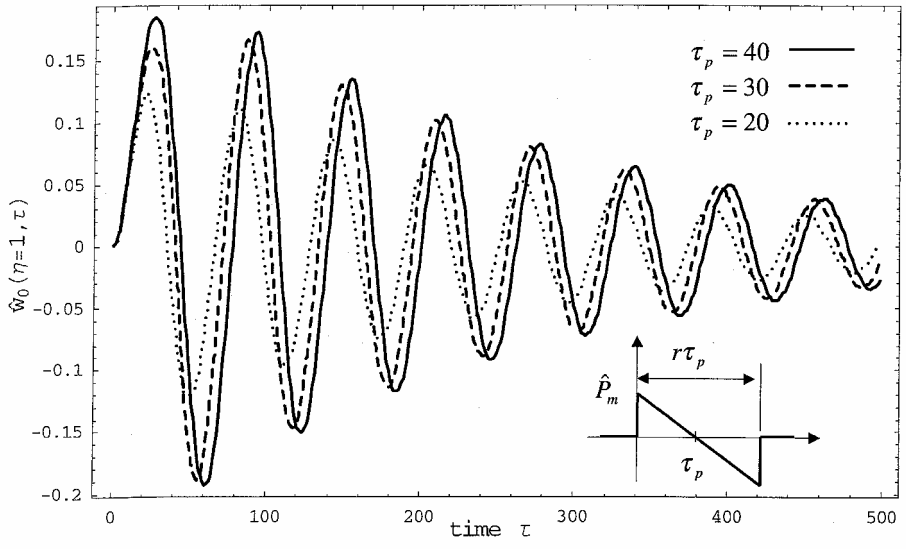

Fig. 11 Response subjected to blast loads with different τ_p, [75$_6$], AR = 16, $\hat{P}_m = 10^{-3}$, r = 1.5, M_F = 0.5, and warping inhibition included.

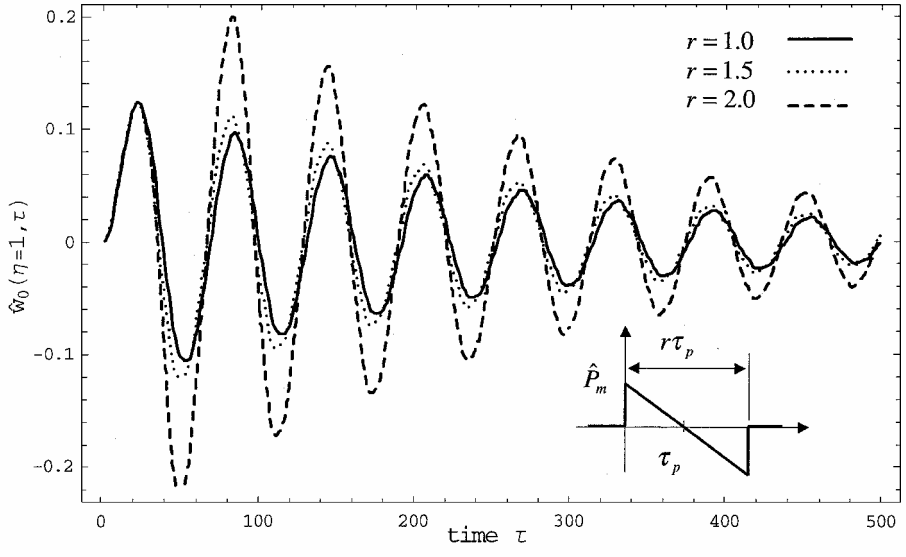

Fig. 12 Response subjected to blast loads with different r, [75$_6$], AR = 16, $\hat{P}_m = 10^{-3}$, τ_p = 20, M_F = 0.5, and warping inhibition included.

V. Conclusions

An efficient and comprehensive aeroelastic model based on an anisotropic thin-walled beam theory and the concept of indicial functions to model the aerodynamic loads in incompressible flow has been proposed and formulated. The theory incorporates a number of nonclassical structural effects. Major conclusions are as follows.

1) The influence of elastic coupling on the aeroelastic response has been quantitatively investigated. It is observed that on one hand, the fluid–wing interaction provides damping to the subcritical response, and on the other hand, it acts as an amplifier to the structural modification due to elastic coupling. For the case studied in the text, one unit structural modification can be amplified to about 3 unit modification of the total response change.

2) For aircraft wings with large aspect ratio ($AR \geq 12$), warping inhibition has marginal influence on the response, even in the presence of amplifing effect of the fluid–structural interaction.

3) Given the peak reflected overpressure $\hat{P}_m$, the blast profile specified by the parameters r and t_p is significant in accurately predicting the maximum amplitude of the response subjected to such types of blast pulses.

The results obtained here are expected to contribute, among others, to the further understanding of the mechanism of aeroelastic tailoring and warping inhibition effect on the response.

Appendix A: Expression of One-dimensional Stiffness and Inertia Coefficients

The global stiffness quantities a_{ij} $(=a_{ji})$ and inertia terms related to the problem are defined as

$$a_{33} = \oint_C \left[z^2 K_{11} + 2z\frac{\mathrm{d}x}{\mathrm{d}s}K_{14} + \left(\frac{\mathrm{d}x}{\mathrm{d}s}\right)^2 K_{44} \right] \mathrm{d}s$$

$$a_{37} = \oint_C \left[zK_{13} + \frac{\mathrm{d}x}{\mathrm{d}s}K_{43} \right] \mathrm{d}s$$

$$a_{55} = \oint_C \left[\left(\frac{\mathrm{d}z}{\mathrm{d}s}\right)^2 K_{22} + \left(\frac{\mathrm{d}x}{\mathrm{d}s}\right)^2 \bar{A}_{44} \right] \mathrm{d}s$$

$$a_{56} = -\oint_C \left[F_w \frac{\mathrm{d}z}{\mathrm{d}s}K_{21} + a(s)\frac{\mathrm{d}z}{\mathrm{d}s}K_{24} \right] \mathrm{d}s$$

$$a_{66} = \oint_C \left[F_w^2 K_{11} + 2F_w a(s) K_{14} + a(s)^2 K_{44} \right] \mathrm{d}s$$

$$a_{77} = \oint_C \psi(s) K_{23}\, \mathrm{d}s$$

where K_{ij} are the reduced stiffness coefficients and $\bar{A}_{44} = A_{44} - (A_{45}^2/A_{55})$.

The inertia coefficients in the Eqs. (35) are defined as

$$b_1 = \oint_C m_0\, \mathrm{d}s, \qquad (b_4, b_5) = \oint_C (z^2, x^2) m_0\, \mathrm{d}s$$

$$b_{14} = \oint_C m_2 \left(\frac{\mathrm{d}x}{\mathrm{d}s}\right)^2 \mathrm{d}s, \qquad b_{15} = \oint_C m_2 \left(\frac{\mathrm{d}z}{\mathrm{d}s}\right)^2 \mathrm{d}s$$

$$(b_{10}, b_{18}) = \oint_C \left[m_0 F_w^2(s), m_2 a^2(s) \right] \mathrm{d}s$$

in which

$$(m_0, m_2) = \sum_{k=1}^{m_l} \int_{h_{(k^-)}}^{h_{(k^+)}} \rho_{(k)}(1, n^2)\, \mathrm{d}n$$

Appendix B: Definition of Matrices in Equation (46)

$$[\boldsymbol{A}] = \begin{bmatrix} \boldsymbol{A}_s & \boldsymbol{B}_s \\ \boldsymbol{B}_a\boldsymbol{A}_s & \boldsymbol{A}_a + \boldsymbol{B}_a\boldsymbol{B}_s \end{bmatrix}, \qquad [\boldsymbol{B}_e] = \begin{bmatrix} \boldsymbol{0}_{m\times 1} \\ \bar{\boldsymbol{M}}_n^{-1} \\ \boldsymbol{D}_2\bar{\boldsymbol{M}}_n^{-1} \\ \vdots \\ \boldsymbol{D}_2\bar{\boldsymbol{M}}_n^{-1} \end{bmatrix}$$

$$\boldsymbol{Q}_g = \frac{1}{8\mu_0}\left\{ \frac{C_{L\phi}}{\pi}\boldsymbol{\Theta}_w^T \int_0^1 \hat{\boldsymbol{\Psi}}_w\, \mathrm{d}\eta + \frac{C_{L\phi}}{4\pi}\boldsymbol{\Theta}_\phi^T \int_0^1 \hat{\boldsymbol{\Psi}}_\phi\, \mathrm{d}\eta \right\} \times \frac{1}{U_n}\left\{ w_G(0)\psi_K(\tau) + \int_0^\tau \frac{\partial w_G(\tau_0)}{\partial \tau_0}\psi_K(\tau - \tau_0)\, \mathrm{d}\tau_0 \right\}$$

$$\boldsymbol{Q}_b = \frac{1}{4b_1 U_n^2}\left\{ 2b\boldsymbol{\Theta}_w^T \int_0^1 \hat{\boldsymbol{\Psi}}_w\, \mathrm{d}\eta \right\} L_b$$

$$[\boldsymbol{A}_s]_{2m\times 2m} = \begin{bmatrix} 0_{m\times m} & \boldsymbol{I}_{m\times m} \\ -\bar{\boldsymbol{M}}_n^{-1}\bar{\boldsymbol{K}}_n & -\bar{\boldsymbol{M}}_n^{-1}\bar{\boldsymbol{C}}_n \end{bmatrix}$$

$$[\boldsymbol{B}_s]_{2m\times nm} = \begin{bmatrix} \boldsymbol{0}_{m\times nm} \\ (1/8\mu_0)\bar{\boldsymbol{M}}_n^{-1}[\alpha_1\boldsymbol{I}_{m\times m} \quad \cdots \quad \alpha_n\boldsymbol{I}_{m\times m}]_{m\times nm} \end{bmatrix}$$

$$[\boldsymbol{A}_a]_{nm\times nm} = \begin{bmatrix} -\beta_1\boldsymbol{I}_{m\times m} & & \\ & \ddots & \\ & & -\beta_n\boldsymbol{I}_{m\times m} \end{bmatrix}$$

$$[\boldsymbol{B}_a]_{nm\times 2m} = \begin{bmatrix} \boldsymbol{I}_{m\times m} \\ \vdots \\ \boldsymbol{I}_{m\times m} \end{bmatrix}_{nm\times m} [\boldsymbol{D}_1 \quad \boldsymbol{D}_2]_{m\times 2m}$$

$$\boldsymbol{D}_1 = \frac{C_{L\phi}}{\pi}\boldsymbol{\Theta}_w^T \left\{ \frac{2}{AR}\tan\Lambda \int_0^1 \hat{\boldsymbol{\Psi}}_w \hat{\boldsymbol{\Psi}}_w'^T\, \mathrm{d}\eta\boldsymbol{\Theta}_w - \int_0^1 \left[\hat{\boldsymbol{\Psi}}_w \hat{\boldsymbol{\Psi}}_\phi^T + \left(\frac{C_{L\phi}}{\pi} - 1\right)\frac{\tan\Lambda}{2AR}\hat{\boldsymbol{\Psi}}_w \hat{\boldsymbol{\Psi}}_\phi'^T\, \mathrm{d}\eta\boldsymbol{\Theta}_\phi \right] \right\} + \frac{C_{L\phi}}{2\pi}\boldsymbol{\Theta}_\phi^T \left\{ \frac{1}{AR}\tan\Lambda \int_0^1 \hat{\boldsymbol{\Psi}}_\phi \hat{\boldsymbol{\Psi}}_w'^T\, \mathrm{d}\eta\boldsymbol{\Theta}_w - \frac{1}{2}\int_0^1 \left[\hat{\boldsymbol{\Psi}}_\phi \hat{\boldsymbol{\Psi}}_\phi^T + \left(\frac{C_{L\phi}}{\pi} - 1\right)\frac{\tan\Lambda}{2AR}\hat{\boldsymbol{\Psi}}_\phi \hat{\boldsymbol{\Psi}}_\phi'^T \right] \mathrm{d}\eta\boldsymbol{\Theta}_\phi \right\}$$

$$\boldsymbol{D}_2 = \frac{C_{L\phi}}{\pi}\boldsymbol{\Theta}_w^T \left\{ 2\int_0^1 \hat{\boldsymbol{\Psi}}_w \hat{\boldsymbol{\Psi}}_w^T\, \mathrm{d}\eta\boldsymbol{\Theta}_w - \frac{1}{2}\left(\frac{C_{L\phi}}{\pi} - 1\right)\int_0^1 \hat{\boldsymbol{\Psi}}_w \hat{\boldsymbol{\Psi}}_\phi^T\, \mathrm{d}\eta\boldsymbol{\Theta}_\phi \right\} + \frac{C_{L\phi}}{2\pi}\boldsymbol{\Theta}_\phi^T \left\{ \int_0^1 \hat{\boldsymbol{\Psi}}_\phi \hat{\boldsymbol{\Psi}}_w^T\, \mathrm{d}\eta\boldsymbol{\Theta}_w - \frac{1}{4}\left(\frac{C_{L\phi}}{\pi} - 1\right)\int_0^1 \hat{\boldsymbol{\Psi}}_\phi \hat{\boldsymbol{\Psi}}_\phi^T\, \mathrm{d}\eta\boldsymbol{\Theta}_\phi \right\}$$

Acknowledgments

The authors wish to express their indebtedness to Piergiovanni Marzocca for helpful discussions and comments. The reviewers' comments definitely improved the quality of this paper.

References

[1]Marzocca, P., Librescu, L., and Chiocchia, G., "Aeroelastic Response of 2-D Lifting Surfaces to Gust and Arbitrary Explosive Loading Signatures," *International Journal of Impact Engineering*, Vol. 25, No. 1, 2001, pp. 41–65.

[2]Meirovitch, L., *Principles and Techniques of Vibrations*, Prentice–Hall, Upper Saddle River, NJ, 1997, pp. 189–194, 206–210.

[3]Song, O., "Modeling and Response Analysis of Thin-Walled Beam Structures Constructed of Advanced Composite Materials," Ph.D. Dissertation, Dept. of Engineering Science and Mechanics, Virginia Polytechnic Inst. and State Univ., Blacksburg, VA, 1990.

[4]Librescu, L., and Song, O., "Behavior of Thin-Walled Beams Made of Advanced Composite Materials and Incorporating Non-classical Effects," *Applied Mechanics Reviews*, Vol. 44, No. 11, Pt. 2, 1991, pp. S174–S180.

[5]Song, O., and Librescu, L., "Free Vibration of Anisotropic Composite Thin-Walled Beams of Closed Cross-Section Contour," *Journal of Sound and Vibration*, Vol. 167, No. 1, 1993, pp. 129–147.

[6]Bhaskar, K., and Librescu, L., "A Geometrically Non-Linear Theory for Laminated Anisotropic Thin-Walled Beams," *International Journal of Engineering Science*, Vol. 33, No. 9, 1995, pp. 1331–1344.

[7]Librescu, L., and Na, S. S., "Dynamic Response of Cantilevered Thin-Walled Beams to Blast and Sonic-Boom Loadings," *Shock and Vibration*, Vol. 5, No. 1, 1998, pp. 23–33.

[8]Na, S. S., "Control of Dynamic Response of Thin-Walled Composite Beams Using Structural Tailoring and Piezoelectric Actuation," Ph.D. Dissertation, Dept. of Engineering Science and Mechanics, Virginia Polytechnic Inst. and State Univ., Blacksburg, VA, 1997.

[9]Rehfield, L. W., Atilgan, A. R., and Hodges, D. H., "Nonclassical Behavior of Thin-Walled Composite Beams with Closed Cross Sections," *Journal of the American Helicopter Society*, Vol. 35, No. 2, 1990, pp. 42–51.

[10]Smith, E. C., and Chopra, I., "Formulation and Evaluation of an Analytical Model for Composite Box-Beams," *Journal of American Helicopter Society*, Vol. 36, No. 3, 1991, pp. 23–35.

[11]Kim, C., and White, S. R., "Thick-Walled Composite Beam Theory Including 3-D Elastic Effects and Torsional Warping," *International Journal of Solids and Structures*, Vol. 34, No. 31–32, 1997, pp. 4237–4259.

[12]Jung, S. N., Nagaraj, V. T., and Chopra, I., "Assessment of Composite Rotor Blade Modeling Techniques," *Journal of the American Helicopter Society*, Vol. 44, No. 3, 1999, pp. 188–205.

[13]von Kármán, T., and Sears, W. R., "Airfoil Theory for Non-uniform Motion," *Journal of the Aeronautical Sciences*, Vol. 5, No. 10, 1938, pp. 379–390.

[14]Bisplinghoff, R. L., Ashley, H., and Halfman, R. L., *Aeroelasticity*, Dover, New York, 1996, pp. 217, 288–293, 397–399.

[15]Katz, J., and Plotkin, A., *Low-Speed Aerodynamics: From Wing Theory to Panels Methods*, McGraw–Hill, New York, 1991, pp. 451–457.

[16]Theodorsen, T., "General Theory of Aerodynamic Instability and the Mechanism of Flutter," NACA Rept. 496, 1935.

[17]Sears, W. R., "Operational Methods in the Theory of Airfoils in Non-uniform Motion," *Jorunal of the Franklin Institute*, Vol. 230, July 1940, pp. 94–111.

[18]Venkatesan, C., and Friedmann, P. P., "New Approach to Finite-State Modeling of Unsteady Aerodynamics," *AIAA Journal*, Vol. 24, No. 12, 1986, pp. 1889–1897.

[19]Karpel, M., "Design of Active Flutter Suppression and Gust Alleviation Using State-Space Aeroelastic Modeling," *Journal of Aircraft*, Vol. 19, No. 3, 1982, pp. 221–227.

[20]Yates, E. C., Jr., "Calculation of Flutter Characteristics for Finite-Span Swept or Unswept Wings at Subsonic and Supersonic Speeds by a Modified Strip Analysis," NACA RM L57L10, 1958.

[21]Rodden, W. P., and Stahl, B., "A Strip Method for Prediction of Damping in Subsonic Wind Tunnel and Flight Flutter Tests," *Journal of Aircraft*, Vol. 6, No. 1, 1969, pp. 9–17.

[22]Palazotto, A. N., and Linnemann, P. E., "Vibration and Buckling Characteristics of Composite Cylindrical Panels Incorporating the Effects of a Higher Order Shear Theory," *International Journal of Solids and Structures*, Vol. 28, No. 3, 1991, pp. 341–361.

[23]Goland, M., and Luke, Y., "The Flutter of a Uniform Cantilever Wing with Tip Weights," *Journal of Applied Mechanics*, Vol. 15, No. 1, 1948, pp. 13–20.

[24]Patil, M. J., and Hodges, D. H., "Nonlinear Aeroelastic Analysis of Composite Aircraft in Subsonic Flow," *Journal of Aircraft*, Vol. 37, No. 5, 2000, pp. 751–760.

[25]Gern, F., and Librescu, L., "Static and Dynamic Aeroelasticity of Advanced Aircraft Wings Carrying External Stores," *AIAA Journal*, Vol. 36, No. 7, 1998, pp. 1121–1129.

[26]Qin, Z., and Librescu, L., "Static and Dynamic Validations of a Refined Thin-Walled Composite Beam Model," *AIAA Journal*, Vol. 39, No. 12, 2001, pp. 2422–2424.

[27]Qin, Z., and Librescu, L., "Static/Dynamic Solutions and Validation of a Refined Anisotropic Thin-Walled Beam Model," AIAA Paper 2002-1394, April 2002.